

Polymer Dispersions as Intermediate State during the Synthesis of Specialty Polymers

Klaus Tauer*, Victor Khrenov

Max Planck Institute of Colloids and Interfaces
Am Mühlenberg, D 14476
Golm, Germany

Summary: Heterophase polymerization in combination with ceric ion redox initiation offers some unique features with respect to the preparation of block copolymers and block copolymer particles. Various kinds of amphiphilic multi-block copolymers as well as electrosterically or sterically stabilized particles are easily accessible. A special feature of these particles is that they may consist of two different hydrophilic blocks and thus, leading to particles with a structured hydrophilic shell. The amphiphilic multiblock copolymers are used to form a new class of polymer dispersions by self-organization so-called polymeric colloidal complexes. In general, the particles of these complexes are structured and exhibit very often multiple morphologies. This principle of formation of polymer colloids is an easy way to prepare particles with an unusual morphology such as Janus-type particles.

Introduction

To the best of our knowledge one of the oldest, if not the oldest, attempt to synthesize block copolymers was carried out via aqueous heterophase polymerization¹⁾. This method consists of a radical polymerization of a water-insoluble monomer that was emulsified in an aqueous solution of a water-soluble monomer. If a growing radical diffuses across the phase boundary and continues to grow block copolymers are formed. The authors used the most important inherent feature of a heterophase polymerization that is the simultaneous existence of hydrophilic and hydrophobic reaction domains. In particular, they tried to prepare poly(acrylic acid)-*b*-polystyrene copolymers. Unfortunately, the solubility of acrylic acid in the styrene phase is considerable, so that not a pure styrene but a styrene-acrylic acid block was formed. It is interestingly to note that this principle is nowadays utilized for many technically important emulsion polymerization recipes to form *in-situ* acrylic or

methacrylic acid rich copolymers in order to improve the latex stability. The same authors described still another approach, which is in principle also used today in several different ways: the utilization of a polymer, which is able to generate radicals. This approach is not restricted to (aqueous) heterophase polymerization. In the particular case polystyrene was prepared by radical polymerization in the presence of carbon tetra bromide as both photo-initiator and chain transfer agent. The second stage polymerization of methyl methacrylate was started again photochemically by cleaving the carbon bromine bond in the polystyrene prepolymer.

In principle, we report here a combination of both routes by utilizing the ceric ion redox mechanism to generate radicals at polymer chain ends that subsequently form during an aqueous heterophase polymerization (first stage of polymerization) polymeric micelles or particles as isolated reaction loci where the further block copolymer formation takes place.

The ceric ion redox mechanism, which is known already for a long time (cf. Figure 1), has been used with low molecular weight alcohols to start the polymerization of vinyl monomers ^{2, 3)}. For the aim of grafting vinyl monomers onto polymeric backbones cellulose or poly(vinyl alcohol) have been used as polymeric reductants as well ⁴⁾. The radical generation by this redox reaction has basically two important advantages if the ceric ion concentration is in an optimum range. Firstly, the redox reaction is fast and hence, the duration of the initiation period is very short. Secondly, it is a process that results in a single radical and hence, primary radical recombination is very unlikely.

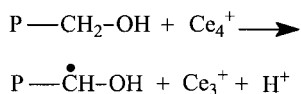


Figure 1: Ceric ion redox mechanism with a hydroxyl methyl group containing polymer as reductant; P symbolizes a polymeric chain.

Of course, if the polymeric reductant (or the prepolymer) is water-soluble and has only one or two reducing groups this kind of initiation reaction is a promising candidate for the preparation of linear block copolymers via aqueous heterophase polymerizations. Note, the type of block copolymer formed (diblock, triblock or multiblock) depends on both the number of radicals per precursor polymer and the termination mode of the monomer. In this sense poly(ethylene glycol) has widely used as reductant to prepare block copolymer latex particles ⁵⁻⁷⁾.

Ceric ion is a strong oxidizing agent and hence, many compounds react with it as reductant. For instance, it is reported that also carboxylic acids ²⁾ can act as reductant as well as organic sulfonates ⁶⁾. However, it is a matter of fact that as soon as methylol groups are present the reaction takes place preferentially as described in Figure 1. This particular behavior is demonstrated by the polymerization results depicted in Figure 2 obtained with N-isopropylacryl amide (NIPAM) ⁸⁾.

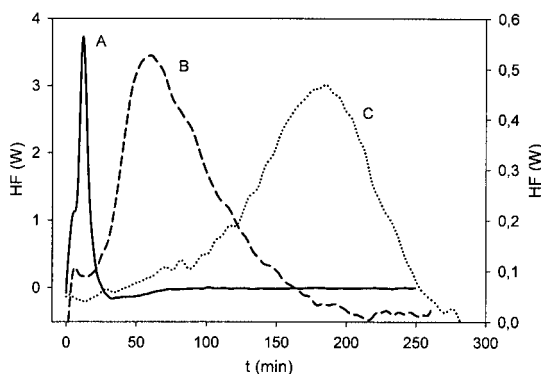


Figure 2: Heat flow (HF) time curves for polymerization of NIPAM.

- A – polymerization started with the redox system Ce^{4+} / PSS-OH (left y-axis)
- B – polymerization started with the redox system PEG-OH (right y-axis)
- C – polymerization started with NIPAM / Ce^{4+} (right y-axis) (cf. text below)

These results clearly show that in the presence of water-soluble prepolymers the heat development starts immediately after the addition of Ce^{4+} that was done at time zero. Curve C in Figure 2 indicates also a polymerization in the absence of the prepolymers but with a considerable delay compared to curves A and B. The behavior of the neat NIPAM was investigated in some detail and it turned out that the reaction profile depends strongly on the purity of the monomer batch. Even a monomer batch that was purified three times by recrystallization from a mixture of benzene and hexane (30:70 = v:v) underwent polymerization but with a maximum in the reaction rate profile at still larger times than curve C in Figure 2. Note, methyl methacrylate (MMA) and styrene do not polymerize without prepolymers over a period of time of several hours. In summary, these results confirm the fast reaction of the ceric ion redox system in the presence of prepolymers with terminal methylol groups. But for some monomers, such as NIPAM, the formation of some substantial

amounts of homopolymer due to the direct reaction of the monomer with the ceric ion cannot be excluded per se but optimizing the reaction conditions can minimize the amount of homopolymer. In general, the behavior of each particular monomer under the conditions of the ceric ion redox initiation has to be investigated in order to avoid disappointments.

This contribution consists of two major parts. The first part highlights the possibilities of the ceric ion redox initiation with polymeric reductants in combination with aqueous heterophase polymerizations with respect to the preparation of unique block copolymers that are not accessible by other procedures. The enormous potential of this method is demonstrated in some detail by means of the preparation and properties of poly(styrene sulfonates)-*b*-poly(*N*-isopropyl acryl amide) (**PSS-PNIPAM**) diblock copolymers, poly(styrene sulfonates)-*b*-poly(*N*-isopropyl acryl amide)-*b*-polystyrene (**PSS-PNIPAM-PS**) tri block copolymers, and poly(ethylene glycol)-*b*-poly(*N*-isopropyl acryl amide)-*b*-poly(methyl methacrylate) (**PEG-PNIPAM-PMMA**) triblock copolymers. Finally, the second part describes the use of a construction set of such different block copolymer to form a special form of polymeric colloids, so called polymeric colloidal complexes (**PCC**).

Experimental Part

Chemicals. All chemicals except the monomers were used as received. The monomers were either carefully distilled or at least two times recrystallized prior to use. Cerium ammonium nitrate from (Fluka) was used as ceric ion source.

Polymerizations. All polymerizations were carried out either in all glass reactors equipped with stirrer, reflux condenser, nitrogen inlet and outlet, heating jacket to control the temperature, and a valve on the bottom to remove the latex or in reaction calorimeter RM200 (ChemiSens AB, Lund, Sweden) as described in detail elsewhere ^{7, 9}. All recipe components except the initiator or the ceric ions were placed in the reactor during the thermal equilibration method and the reaction was started by injecting an aqueous solution of the initiator or ceric ions. All polymerizations were allowed to run until complete conversion. For the detailed polymerization recipes see the corresponding caption of the Figures and the text. The reaction products were ultrafiltrated through a regenerated cellulose membrane with a cut-off of 10 kD (Millipore, Bedford, USA) with at least the 10-fold amount of distilled water in order to remove unreacted monomers and inorganic salts.

Preparation of PCC. The PCC formation took place immediately after mixing aqueous solution of the corresponding components of proper concentrations (1 wt-% for the polymers and 2 wt-% for the surfactants). To remove unreactive material and counterions the PCC dispersions were dialyzed against the 10-fold amount of distilled water. The cut-off of the dialysis tubing was $1.4 \cdot 10^4 \text{ g mol}^{-1}$ (Visking, type 36/32, Carl Roth GmbH Karlsruhe, Germany). The water was replaced daily until its conductivity was constant. This took about 450 hours for all samples independent of the particular composition. In order to get solids the PCC dispersions were freeze-dried (Christ LMC-2, Germany) after dialysis.

Characterization methods. Polymer and latex characterizations were carried out by standard procedures such as gel permeation chromatography (Thermo Separation Products set-up being equipped with UV (TSP UV1000) and RI (Shodex RI-71) detectors in THF at 30 °C with a flow rate of 1 ml per minute. A column set was employed consisting of three 300 x 8 mm columns filled with a MZ-SDplus spherical polystyrene gel (average particle size 5 μm) having a pore size of 10^3 , 10^5 , and 10^6 \AA , respectively), elemental analysis (vario EL elemental analyzer, Analysensysteme GmbH, Hanau, Germany), dynamic light scattering with a NICOMP particle sizer (model 370, NICOMP particle sizing systems, Santa Barbara, California, USA), and transmission electron microscopy (TEM) Zeiss EM 912 Omega operating at 100 kV; samples were prepared by suspension preparation onto carbon-coated copper grids). For atomic force microscopy (AFM) imaging a nanoscope III MultiMode system (Digital Instruments, Santa Barbara, CA, USA) was used. Measurements were carried out in the TappingModeTM utilizing silicon cantilevers (42 N/m, Olympus optical Co. Ltd., Japan) at resonance frequencies of 250-280kHz under ambient conditions. For selected samples dynamic and static light scattering investigations were carried out simultaneously with a goniometer ALV/SP-86#057 (ALV, Langen, Germany) in order to determine the radius of gyration (R_g) and the hydrodynamic radius (R_h) from static and dynamic ZIMM plots, respectively. A Nonius rotating anode device ($P = 4 \text{ kW}$, $\text{CuK}\alpha$) and an image-plate detector system were used for the small angle X-ray scattering (SAXS) measurements. With the image plates placed at a distance of 40 cm from the sample, a scattering vector range from $s = 0.05 - 1.6 \text{ nm}^{-1}$ ($s = 2/\lambda \sin \theta$) was available. The samples were irradiated for 18 h to reduce the noise level and to obtain a sufficiently high scattering intensity. The 2D isotropic diffraction patterns were transformed into a 1D

radial average of the scattering intensity X-ray. The glass transition temperature was determined with a TG 209 (Netzsch, Germany) according to standard procedures.

Results

Block copolymers and block copolymer particles – Preparation and Properties

The confined reaction loci of a micelle – a key result

During a systematic investigation of the polymerization of NIPAM with the Ce^{4+} / PEG redox system a really surprising effect was found^{10, 11)}. The result of this key experiment that has been proved meanwhile several times by other experimenters is depicted in Figure 3¹²⁾. These results clearly show that after finishing the polymerization of the initial batch of monomer at about 50 minutes further monomer, which was added at points 2 and 3, can be polymerized without the addition of new initiator. Note, up to 5 monomer additions over a time period of 20 hours could consecutively be polymerized when the reaction system was kept at 60 °C. However, if together with the monomer a few milligrams of ferrous chloride were added no polymerization was observed (cf. curve B in Figure 3). From former results^{10 - 13)} it is known that the ceric ion reaction with the PEG is completed within the first 10 minutes of the reaction. Consequently, the results depicted in Figure 3 prove that radicals can survive a considerable period of time (up to some ten hours) in the confined reaction space of PEG-PNIPAM micelles (or particles) that are formed shortly after the start of the polymerization due to the lower critical solution temperature (LCST) of the PNIPAM block.

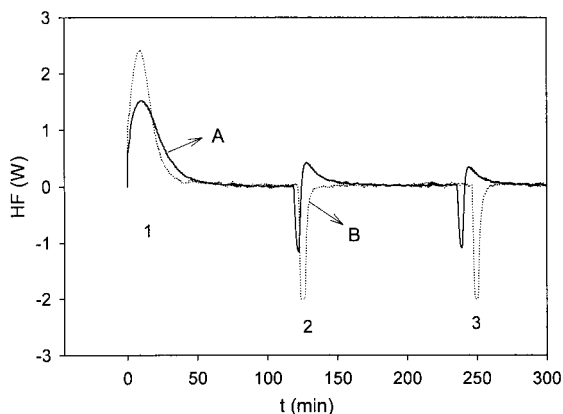


Figure 3: Heat flow time curves for a polymerization of NIPAM initiated with PEG / Ce^{4+} .

Curve A – at events 2 and 3 repeated addition of 0.9g and 0.7 g of NIPAM, resp., dissolved in 4 g of water

Curve B - at events 2 and 3 repeated addition of 0.9g of NIPAM and some mg of FeCl_2 dissolved in 4 g of water.

Furthermore, the suppression of any polymerization in the presence of ferrous ions leads to the conclusion that an intense exchange between the aqueous phase (at least of low molecular weight species) and the hydrophobic core of the micelles / particles ¹⁴⁾ exists.

Indeed, the data shown in Figure 3 are a second key result besides that depicted in Figure 2. Both data sets describe prerequisites in order to prepare multiblock copolymers via radical polymerization in aqueous heterophase systems. The first requirement is the fast redox reaction between ceric ions and terminal methylol - groups in polymers (cf. Figure 2) and the other requirement is the long lifetime of radicals in PEG-PNIPAM micelles (cf. Figure 3). Note, the second requirement bases on the first and leads actually in any case to triblock copolymers. However, if PEG is used as polymeric reductant (prepolymer) this block is usually much shorter than the other blocks but nevertheless it is present in the final product.

Poly(styrene sulfonates)-b-poly(N-isopropyl acryl amide) diblock copolymers

The preparation of these diblock copolymers is comparatively simple as illustrated above (curve A in Figure 2). The PSS-PNIPAM copolymers are thermosensitive i.e., they form at elevated temperature electrosterically stabilized micelles. This behavior is demonstrated in Figure 4 by means of the average particle size (intensity weighted diameter, D_i) determined by dynamic light scattering at different temperatures. It is to be seen that this copolymer forms a clear solutions at 25 °C and still at 30 °C but becomes turbid and forms a dispersion between 30 and 35 °C. The LCST of the copolymer is obviously almost unchanged compared with the homo-PNIPAM.

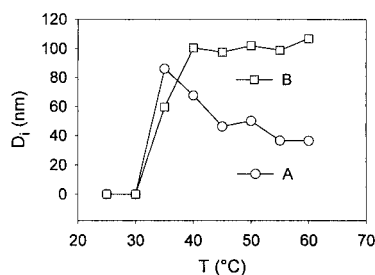


Figure 4: The thermosensitive behavior of a PSS-PNIPAM diblock copolymer (curve A) in comparison with a PNIPAM homopolymer (curve B).

However a further increase in the temperature leads to a distinct difference between the copolymer and the homopolymer. The average size of the copolymer micelles decreases whereas the size of the homopolymer aggregates slightly increases. The number of the latter decreases due to coagulation processes. Note, the collision frequency between the ag-

gregates is increased the higher the temperature. Contrary, the number of electrosterically stabilized micelles decreases with increasing temperature due to the stronger repulsion of the charged blocks.

Solutions of PSS-PNIPAM block copolymers are not only sensitive against temperature increase but also if the ionic strength in the aqueous phase is increased the PNIPAM block becomes insoluble. The aggregation behavior upon the addition of sodium chloride at temperature of 25 °C is shown in Figure 5.

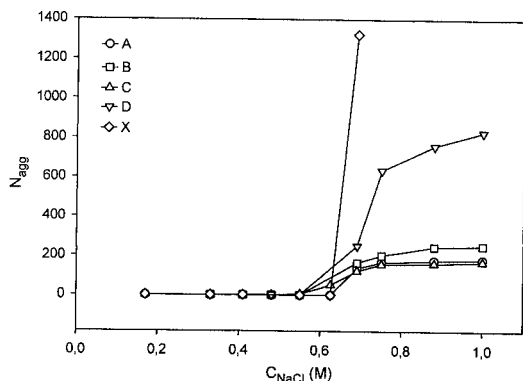


Figure 5: Aggregation number (N_{agg}) of PSS-PNIPAM block copolymers of different molecular weight (A-D, cf. Table 1) and a simple mixture of PSS and PNIPAM (X) in dependence on NaCl concentration.

Table 1. Molecular weight (MW_{LS}) from static light scattering of PSS-PNIPAM block copolymers prepared with different cerium ammonium nitrate concentrations (C_{Ce})

Run (cf. insert Fig.5)	C_{Ce} (M)	MW_{LS} ($g\ mol^{-1}$)	MW_{PNIPAM} ($g\ mol^{-1}$) ^{a)}
A	$5 \cdot 10^{-4}$	$13.0 \cdot 10^5$	$9.1 \cdot 10^5$
B	$2 \cdot 10^{-3}$	$7.9 \cdot 10^5$	$4.0 \cdot 10^5$
C	$4 \cdot 10^{-3}$	$9.0 \cdot 10^5$	$5.1 \cdot 10^5$
D	$2 \cdot 10^{-2}$	$2.0 \cdot 10^5$	/

a) MW_{PNIPAM} – molecular weight of the PNIPAM block calculated from MW_{LS} and the molecular weight of the PSS precursor that was $3.9 \cdot 10^5\ g\ mol^{-1}$

The onset of the aggregation occurs independent of the particular sample at a sodium chloride concentration between 0.5 and 0.6 M. The results summarized in Figure 5 and Table 1 lead immediately to some important conclusions. Firstly, the aggregation is entirely due to the behavior of the PNIPAM block as the simple mixture of the corresponding homopolymers starts to aggregate in the same concentration range. Secondly, the aggregates are stabilized by the PSS blocks that prevent macroscopic aggregation as it takes place in the case of the simple mixture (X in Figure 5). Thirdly, the aggregation number is almost independent of the molecular weight of the PNIPAM block for a given PSS block. Note, that for sample D the high ceric ion concentration leads to a chain scission of PSS precursor polymer (cf. Table 1). This is obviously the main reason for the higher aggregation numbers. Fourthly, The aggregates are stable up to high sodium chloride concentrations thus indicating electrosteric stabilization by the PSS blocks. Note, in the simple mixture the PSS polymers are unable to stabilize the PNIPAM aggregates.

In summary, the use of PSS with methylol terminal groups as reductant for ceric ions allows the preparation of block copolymers in aqueous media such as PSS-PNIPAM block copolymers. These block copolymers show both temperature and electrolyte induced micellization. The micelles are electrosterically stabilized by the PSS blocks that keep stretched into the aqueous phase upon temperature increase and salt addition.

Poly(styrene sulfonates)-b-poly(N-isopropyl acryl amide)-b-polystyrene triblock copolymers

A similar procedure as described in Figure 3 for the consecutive polymerization in PEG-PNIPAM micelles can also be applied in the case of PSS-PNIPAM micelles described above. Figure 6 shows conversion - time - curves for styrene polymerizations in PSS-PNIPAM micelles. Styrene monomer was added 40 and 90 minutes after the start of the NIPAM polymerizations for runs A-C and D, respectively. At this time the NIPAM polymerization was completed (cf. Figure 2) ¹⁵⁾. The data illustrate that the kinetics of the styrene polymerization depends strongly on the amount of NIPAM that was used during the first polymerization. Decreasing the amount of NIPAM by a factor of 4 leads to a considerable deceleration of the second stage styrene polymerization (cf. runs A and C in Figure 6). This is a reasonable result since the lower the NIPAM concentration the smaller the micelles and the lower is the number of radicals that can survive in the PSS-PNIPAM micelles.

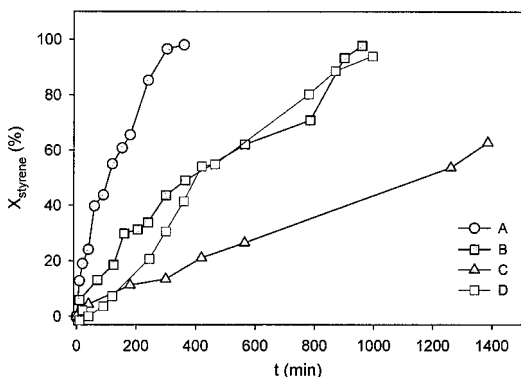


Figure 6: Development of the styrene conversion (X_{styrene}) during the polymerization PSS-PNIPAM micelles¹⁵⁾.

A - 0.055 M NIPAM

B - 0.028 M NIPAM

C - 0.014 M NIPAM

D - 0.028 M NIPAM

A comparison of the curves for runs A-C with that for run D reveals that the period of time between the start of the polymerization and the second monomer addition has only a minor (almost no) influence on the kinetics of the polymerization. The NIPAM concentration and hence, the properties of the PSS_PNIPAM micelles have a much stronger influence.

The final result of these polymerizations is “hairy” polystyrene latexes that are at temperatures below the LCST of the PNIPAM block stabilized by both the PNIPAM (steric stabilization) and the PSS (electrosteric stabilization) blocks that are stretched into the aqueous phase.

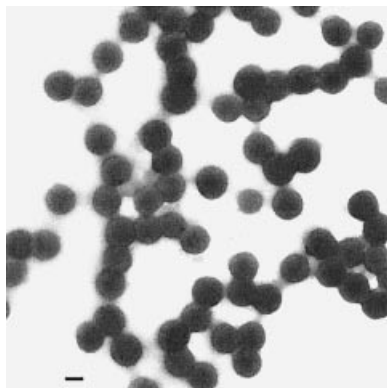


Figure 7: TEM picture of the final polystyrene latex prepared according to run B as described in Fig.5.

The bar indicates 200 nm.

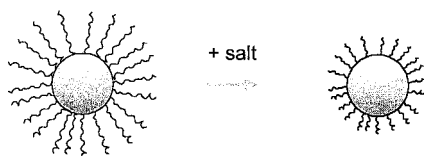
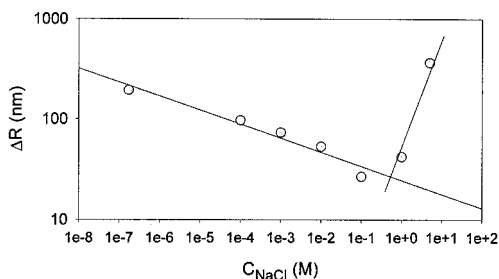
Note, these particles show an increasing photographic blackening at the edges. This dark etch is due to the collapsed PSS and PNIPAM blocks that have a higher electron density compared to PS. “Normal” PS particles show a decreasing photographic blackening at the edges.

Table 2. summarizes the results of the quantitative characterization of the particles prepared according to runs A and B as described in Figure 6 by dynamic light scattering and by enumeration of about 1000 particles on TEM pictures.

Table 2: Characterization of PSS-PNIPAM-PS triblock copolymer particles ¹⁶⁾

Run	$D_{1,0}$ (nm)	$D_{1,3}$ (nm)	$D_{3,3}$ (nm)	D_i (nm)	$D_{1,3}/D_{1,0}$	ΔR (nm)
A	201.2	209.9	212.7	884	1.043	335.5
B	311.6	319.8	322	709	1.026	193.5

These results reveal that the PSS-PNIPAM-PS triblock particles appear on the TEM pictures in the dried state, i.e. when the hairs are collapsed onto the PS-core, quiet monodisperse as the ratio $D_{1,3}/D_{1,0}$ reveals. On the other hand, these particles possess a very huge corona in the order of a few hundreds of nanometers. Particles of this type are called “porcupine” particles and possess an extraordinary electrolyte stability as it was theoretically predicted ¹⁷⁾ and experimentally confirmed ¹⁸⁾. The increased electrolyte stability compared to purely electrostatically stabilized particles is basically due to the possibility of the polyelectrolyte blocks in the corona to be compressed upon increasing the ionic strength. This change of the particles is sketched in Figure 8a whereas experimental results are shown in Figure 8b. The electrolyte stability was determined by dynamic light scattering of latex samples diluted with sodium chloride solutions of the corresponding concentrations. About 1 μ l of latex was diluted with 10 ml of sodium chloride solution to get the necessary count rate for the dynamic light scattering measurements. ΔR was calculated for each concentration with the actual D_i as described above.

**Figure 8a:** Sketch of the behavior of polyelectrolyte decorated particles upon salt addition.**Figure 8b:** Decrease of the corona thickness of PSS-PNIPAM-PS triblock copolymer particles (run B of Fig.6) upon the addition of NaCl.

The compression of the corona thickness with an increase in the sodium chloride concentration over almost seven orders of magnitude is clearly to be seen. The particles start to aggregate at a NaCl concentration of about 0.9 M (indicated by an increasing ΔR which is due to the formation of aggregates, i.e. D_i starts to increase at this salt concentration). Note, purely electrostatically stabilized polystyrene particles (sodium dodecylsulfate as emulsifier) start to coagulate at sodium chloride concentration of about $5 \cdot 10^{-2}$ M.

Poly(ethylene glycol)-b-poly(N-isopropyl acryl amide)-b-poly(methyl methacrylate) triblock copolymers

The synthesis of this triblock copolymer particles that are supposed to be completely uncharged (at least after the ultrafiltration step) has been carried out as described by the reaction rate profile depicted in Figure 9. This is a description of the whole polymerization experiment in the reaction calorimeter¹⁹⁾. Period 1 is the phase of thermal equilibration where the calorimeter is filled with water, NIPAM monomer, and PEG-monomethylether. During period two the system is calibrated with a thermal power of 2 W. After the calibration power is switched off and a short period of re-equilibration the polymerization is started by injecting a solution of cerium ammonium in nitric acid at point A. Then, during interval 3 the polymerization of the NIPAM takes place.

During interval 3 the reaction mixture becomes shortly after the addition of the ceric ions turbid. However, if the reaction would have been stopped at the end of interval 3 the PEG-PNIPAM micelle dissolve again upon cooling down to room temperature. Interval 4 is the MMA polymerization, which was added at point B. At the end of the polymerization, after about 5 hours, stable PEG-PNIPAM-PMMA triblock copolymer latex is removed from the reactor, which does not resolve upon cooling down.

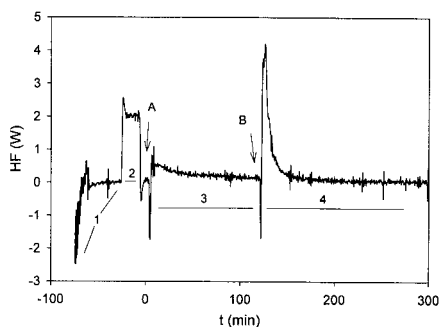


Figure 9: Calorimetric reaction protocol of the preparation of PEG-PNIPAM-PMMA triblock copolymers.

The time axis is set to zero at the start of the reaction when the polymerization was started by adding the ceric ions.

A similar procedure as described in Figure 9 can be carried with styrene or 2-acrylamidopropanesulfonate as second monomer during interval 4. Only in the latter case the dispersion will change into a highly viscous solution upon cooling down to room temperature. In this particular case the block copolymer consists of three hydrophilic but chemically different blocks. In analogy to the double hydrophilic block copolymers (PEG-PNIPAM or PSS-PNIPAM) this type can be called triple hydrophilic block copolymer.

The results of a systematic study regarding the influence of the ceric ion concentration on the second stage polymerization are summarized in Figure 10. The maximum polymerization rate depends strongly of the cerium ammonium nitrate concentration and hence, on the number of radicals formed during the first stage polymerization. Note, at concentration of ceric ions below 2 mM the number of radicals that have survived the first polymerization is too low to start the second polymerization.

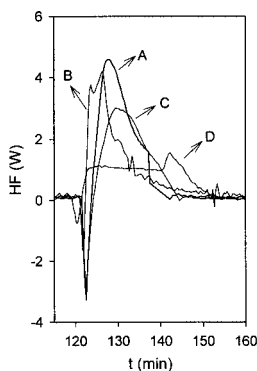


Figure 10: Reaction rate profiles for the second stage polymerization of the procedure as described in Fig.9 but with various amounts of cerium ammonium nitrate.

- A – 14 mM Ce^{4+}
- B – 7 mM Ce^{4+}
- C – 5.2 mM Ce^{4+}
- D – 3.5 mM Ce^{4+}

These PEG-PNIPAM-PMMA triblock copolymer particles can be considered in principle as uncharged hairy particles but not in analogy to the PSS-PNIPAM-PS particles as uncharged “porcupines”. The corona of the PEG-PNIPAM-PMMA triblock copolymer particles behaves completely different upon electrolyte addition compared to the “porcupine” particles (cf. Figure 11). The corona thickness of the uncharged particles increases very slightly while that of the “porcupine” particles decreases by a factor of almost 5 as a result of the compression of the stretched PSS chains. Note, the PEG-PNIPAM-PMMA particles start to coagulate at a NaCl concentration between 10^{-1} and 1 M, which is the same range where the PSS-PNIPAM micelles are formed (cf. Figure 5).

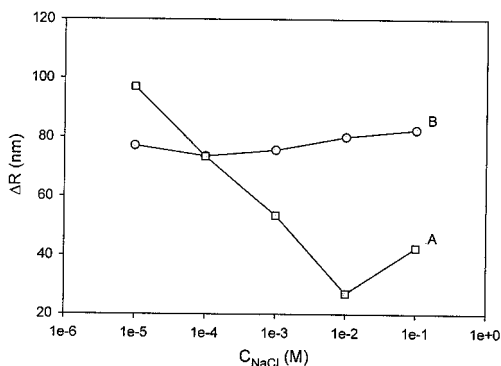


Figure 11: Change of the corona of charged and uncharged triblock copolymer particles in dependence on the sodium chloride concentration.

A – PSS-PNIPAM-PS, charged particles

B – PEG-PNIPAM-PMMA, uncharged particles

At a NaCl concentration above 0.6 M the PNIPAM blocks collapse onto the cores and the triblock particles lose their stability. The short PEG chains are obviously not able to prevent coagulation at this electrolyte concentration.

A detailed discussion of the morphology of any kind of hairy particles requires distinguishing between the “dry” state (isolated particles in vacuum or air such as for TEM or AFM investigations) and the “wet” state (isolated particles in a liquid dispersion such as during light scattering investigations). In the dry state the PEG-PNIPAM-PMMA particles look almost spherical with a very narrow particle size distribution (cf. Figures 12 and 13). The almost monodisperse particle size distributions for both types of triblock copolymer particles (cf. Figure 7) strongly suggests that these are thermodynamic equilibrium structures. Furthermore, the TEM and the AFM pictures reveal some surprising details at closer inspection.

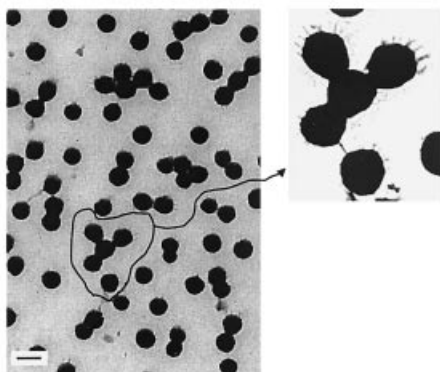


Figure 12: TEM picture of PEG-PNIPAM-PMMA triblock copolymer particles prepared as described in Fig.9; the bar indicates 200 nm; the arrow points to an enlargement of the particular region.

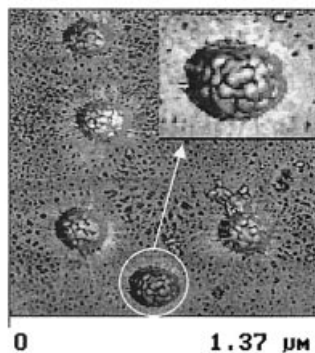


Figure 13: AFM phase image of PEG-PNIPAM-PMMA triblock copolymer particles prepared as described in Fig.9; the particle size is about 200 nm; the arrow points to an enlargement of the particular region.

Under the conditions of TEM investigations the particles appear to be smaller compared with the AFM results. Enumeration of about 1000 particles on TEM pictures results in $D_{1,0} = 145.4$ nm, $D_{1,3} = 146.6$ nm, and $D_{3,3} = 147.0$ nm while on the AFM image the particles are about 200 nm in diameter. This difference of 60 nm is too large to be due to the experimental scatter between both techniques. Furthermore, the particles on the AFM images appear to be slightly out of shape whereas the particles on the TEM pictures are spherical. In general, the structure of the particles under the conditions of AFM is compared to that of the TEM more loosely. It is likely that the particles during the AFM investigations are swollen by the humidity of the air. In contrast, the high vacuum conditions in the electron microscope may cause the particles to shrink and may explain the above differences. Another striking difference between both methods is clearly to be seen in the morphology of the particles. On TEM pictures each particle appears to be hairy (cf. enlarged region of Figure 13), i.e. polymer bundles with a length between 25 - 70 nm and a thickness of about 10 - 15 nm are stretched away from the particle's core. The distance between two such bundles is about 30 - 40 nm. These are of course only rough estimates however; they clearly show that the "hairs" are by no means single polymer chains but very likely composed of several polymer molecules.

On the AFM images the particles show a completely different morphology. There are no bundles stretching away but rather a tuber-like morphology is visible. This morphology is obviously due to phase separation when the double hydrophilic PEG-PNIPAM part of the triblock copolymer collapses during drying onto the PMMA core. Note, in former AFM investigations of PEG-PS diblock copolymer particles a smooth particle surface was observed but ultrasonication revealed phase separated morphologies inside the core of these particles ⁷⁾.

Besides the chemical distribution, which is a characteristic feature in both the "dry" and the "wet" state, block copolymer nanoparticles possess at least under "wet" conditions also a characteristic radial density distribution. This is especially true for both, charged and uncharged hairy particles where the radial density distribution is on the one hand to some extent comparable with star or hyperbranched polymers ²⁰⁾ and microgel particles on the other hand ^{21, 22)}.

The most valuable information with respect to the inner or radial structure of these systems in the dispersed state is obtained from combined dynamic and static light scattering investi-

gations by the so-called P ratio ($P = R_g/R_h$)²³). However, the radial density may change if external stimuli are applied such as changes in the ionic strength (cf. Figure 5) or temperature (cf. Figure 4). In the particular case of the PEG-PNIPAM-PMMA particles the P ratio is expected to depend strongly on the temperature due to the thermosensitive properties of the PNIPAM middle block. Indeed, such a behavior is observed experimentally as it is shown in Figure 14.

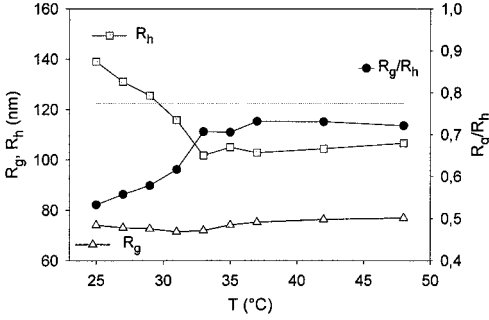


Figure 14: Temperature dependence of R_g , R_h and R_g/R_h for PEG-PNIPAM-PMMA triblock copolymer particles prepared as described in Fig.9.

The gray line corresponds to the P ratio of monodisperse solid spheres ($R_g/R_h = 0.775$).

For a discussion of these dependencies it is helpful to bear in mind that R_g is a geometrical average over the particle size (average distance between the center of mass and the axis of rotation) while R_h is the effective radius acting during motion of the particles. Thus, the P-ratio depends mainly on the radial density distribution of the particles.

The particular situation of the PEG-PNIPAM-PMMA triblock copolymer particles based on molecular and particle parameters is sketched in Figure 15a. The degree of polymerization determined from GPC relative to polystyrene standards (for the PNIPAM and the PMMA blocks) of the PEG, the PNIPAM, and the PMMA blocks are 112, 1640, and 4700, respectively. The core radius (R_c) is 65.5 nm (from TEM and GPC) and the overall corona thickness is 74.5 nm and 39.5 nm below and above the LCST of the PNIPAM (from light scattering, cf. Figure 13), respectively. Figure 15b shows results of model calculation how density profiles of the particles may change upon heating. Note, the R_h/R_c ratio where $\rho(r)$ for curve C and B reaches zero is the corresponding experimental value below and above the LCST of the PNIPAM block, respectively. The depicted $\rho(r)$ curves result in P-ratios of 0.572 (curve C) and 0.616 (curve B). These values fit well to the experimental data (cf. Figure 14). Curve A and D correspond to model cases of hard spheres and particles with still larger corona.

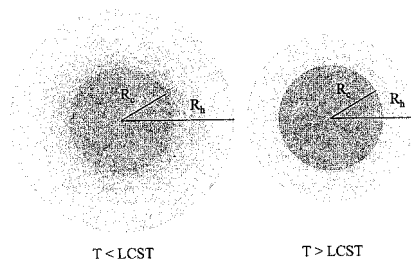


Figure 15a: Sketch of the change of the dimension of PEG-PNIPAM-PMMA particles upon heating above the LCST of the PNIPAM block; R_c / R_h corresponds to light scattering data.

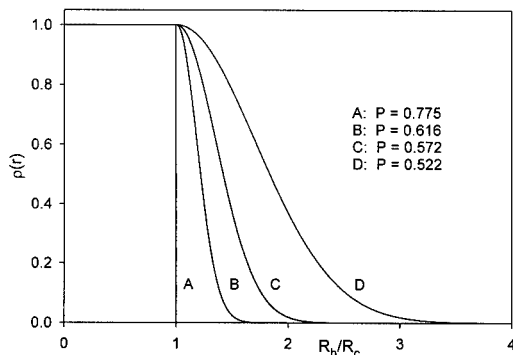


Figure 15b: Model density profiles for hard spheres (A) and hairy particles with varying corona thickness (B – D); P ratios were calculated according to standard equations by means of numerical integration.

Block copolymers via radical heterophase polymerizations – a preliminary summary

The results presented show that aqueous heterophase polymerization is indeed very well suited to prepare special block copolymers which are not or at least not easy accessible by other polymerization techniques. A special advantage of the heterophase technique is the comparatively easy access to a variety of amphiphilic block copolymers. Table 3 gives a selection of block copolymer prepared so far.

Table 3: List of block copolymers prepared via aqueous heterophase polymerization

#	Block copolymer	#	Block copolymer
V40	PSS - PNIPAM	V76Ra	PEG - PNIPAM - PAMPS
V45	PDEAEMA ^{a)} - PNIPAM	V90	PDEAEMA - PMMA
V49	PAMPS ^{b)} - PNIPAM	V98	PSS - PNIPAAm - PS
V62	PNVPn ^{c)} - PNIPAM	V98.18	PSS - PNIPAM - P(EA - co - MAA) ^{d)}
V67	PEG - AMPS	V100	PSS - PtBMA ^{e)} / PSS - PMAA ^{f)}
V68	PEG - DEAEMA	V105	PSS - PNIPAM - PGMA ^{g)}
V75	PEG - PNIPAM - PS	V111	PSS - PMMA / PSS - PS
V76	PEG - PNIPAM - PMMA	V116	PMMA - PAA ^{h)}

a) – poly(diethylamino-ethyl methacrylate); b) – poly(2-acrylamidopropane sulfonate);

c) – poly(N-vinyl pyrrolidon); d) – poly(ethyl acrylate-co-methacrylic acid);

e) – poly(t-butyl methylacrylate); f) - poly(methacrylic acid);

g) – poly(glycidyl methacrylate); h) - poly(acrylic acid)

Besides amphiphilic block copolymers the selection in Table 3 contains also some double hydrophilic or triple hydrophilic block copolymers. A special feature of the triblock copolymer particles is that two differently hydrophilic polymer blocks stabilize them. These are to the best of the authors' knowledge the first examples with this new kind of sterical stabilization. Note, the possible block copolymers structures that are accessible are by no means complete by this list.

There are important questions to be considered regarding the molecular structure and the copolymer yield. Sure, the molecular structure of these block copolymers is less well defined than that of polymers prepared by living polymerization techniques. This is mainly due to two facts. Firstly, radical polymerizations are prone to side reactions what is a general problem that is still enhanced in aqueous reaction medium. Secondly, there is in most radical polymerizations not only a single termination mode. Disproportionation and recombination leads to different types of block copolymers with respect to the number of blocks per molecule and hence, a block copolymer mixture (diblocks, triblocks, and multiblocks) can be formed ⁷⁾.

The overall block copolymer yield is mainly determined by the percentage of radicals that survive in the micelles during the first polymerization. During the second polymerization the block copolymer yield is governed by the probability of chain transfer reactions. A clear estimation of the block copolymer is complicated by the fact that each block that is prepared by radical polymerization has a broad molecular weight distribution. Consequently, the procedure employed inevitable also leads to broad block length or chemical distribution. This fact complicates the analytics and characterization considerably because a copolymer with a long A and a short B block behaves almost like a homopolymer of A and vice versa.

Although a long period of time has passed between the first idea of Dunn and Melville ¹⁾ and a more detailed re-investigation of the capabilities of heterophase polymerization techniques the limits of these approach are not yet reached today. The summary has to be preliminary because a lot of things are still necessary to do. Furthermore, the preparation of block copolymers via radical heterophase polymerization is far from being optimized.

Polymeric colloidal complexes – preparation and properties

PCC - a special type of polymer colloids

If once a construction set of different amphiphilic, double hydrophilic or triple hydrophilic block copolymers (or the corresponding particles), such as described above, is available, these polymers can be used in miscellaneous experiments. An interesting utilization of such substances is the formation of complexes via self-organization simply by mixing the components in a proper range of concentrations. These complexes are expected to have properties different than the starting materials. For instance mixing or “self-organizing” of a double hydrophilic block copolymer with one negatively charged block with another where the charged block is cationic leads to the formation of a polyelectrolyte complex (via electrostatic interactions) that is stabilized by the remaining uncharged hydrophilic blocks. If both uncharged hydrophilic blocks are chemically different the stabilizing layer of the polyelectrolyte complex formed consists of chemically different areas. This is a comparatively easy way to form a special kind of so-called *Janus* particles²⁴⁻²⁷⁾, namely double hydrophilic *Janus*-particles. On the other hand these particle can be considered also as a special kind of polymer dispersions as it is elucidated by the scheme in Figure 16. This scheme is based on the definition of polymer dispersion as any kind of polymer particles with colloidal dimensions that are dispersed in a liquid continuous phase. In this sense so-called artificial latexes, block copolymers in selective solvents, and PCC clearly belong to the group of polymer dispersions. A polymer dispersion is called a *primary dispersions* when the polymer is directly synthesized in form a polymer dispersions i.e. by one of the heterophase polymerization techniques or as natural latex in the *hevea brasiliensis* tree. Polymers that are prepared by other polymerization techniques can be converted into a secondary polymer dispersion by several procedures.

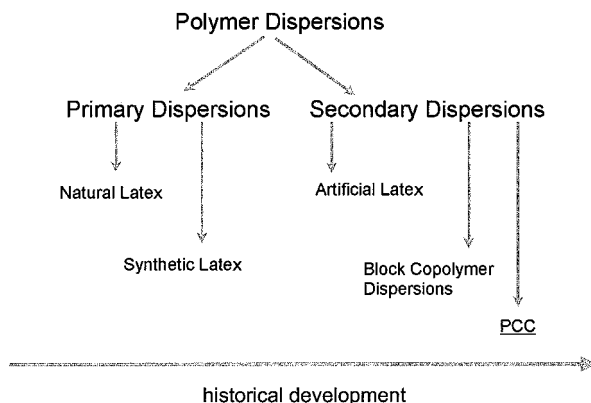


Figure 16: A family tree polymer dispersions where the order from left to right describes the historical development.

If the polymer is dissolved and the solution is subsequently emulsified into another liquid that is a nonsolvent for these solutions so-called artificial latexes are obtained. In this sense also block copolymers in a selective solvent belong to this class of polymer dispersions.

Note, PEG-PNIPAM and PSS-PNIPAM diblock copolymers alone can also form PCC either if the temperature is above the LCST of PNIPAM block (cf. Figure 4) or if the sodium chloride concentration is higher than 0.6 M (cf. Figure 5). In these cases induced hydrophobic interactions lead instead of the above-mentioned electrostatic interaction to the self-organization of chemically identical molecules. Note, micellization is an absolutely comparable process. Other examples of this kind of PCC formed via hydrophobic interactions are all of the above mentioned triblock copolymer particles.

Table 4 contains a selection of PCC formed by interaction of two components via electrostatic interactions.

The data in Table 4 contain three important results. First, the complex formation takes place with a 1:1 stoichiometry as indicated by #2,3,5. Second, the complexes show all two glass transition temperatures where the higher one is that of the complex block. These data suggest that the T_g of the stabilizing block depends on the composition of the complex block.

Third, the average particle size can be varied over a wide range and depends strongly on the partners forming the complex.

Table 4: Characterization of PCC with respect to composition, glass transition temperature (T_g), and average particle size (D) after dialysis ²⁸⁾

#	Components	S / N ^a	T_g (°C)	D (nm) ^b
1	PEG - PDADMAC ^c / PSS - PNIPAM	0.279	33 / 113	190
2	PEG - PSS / CTAB ^d	2.342	40 / 163	11400
3	PEG - PDADMAC / E30 ^e	2.310	22 / 130	310
4	PEG - PDADMAC / PSS - PNIPAM	0.252	48 / 138	180
5	PEG - PSS / PEG – PDADMAC ^f	2.320	34 / 109	26000
6	PSS - PNIPAM / PDEAMA - PNIPAM	0.381	/	275

a – weight ratio sulfur to nitrogen; S/N = 2.289 means a 1:1 stoichiometry; b – intensity weighted average from NICOMP; c – poly(diallyl dimethyl ammonium chloride); d – cetyl trimethyl ammonium chloride; e – sodium alkylsulfonate with an average carbon chain length of C₁₅; f – in this case the PSS – PNIPAM block copolymer possess a comb-like structure as the PSS had no methylol terminal groups and the polymerization was started via a redox reaction between the ceric ion and the styrene sulfonates units as described in ⁶⁾

The appearance of these PCC is absolutely comparable with that of normal polymer dispersion i.e., they are milky white with an apparently low viscosity. Note, after freeze-drying the PCC solids are very easily to redisperse in water. Among all the combinations we have looked at so far PCC#3 in Table 4 (PEG - PDADMAC / E30) behaves in a very special way. This PCC dispersion shows a streaming birefringence that is a typical behavior of lamellar phases such as it is known for surfactant bilayers ²⁹⁾. Note that the corresponding „mirror“ PCC#2 in Table 4 does not show streaming birefringence. This already indicates a difference with regard to the structural order in both complexes. The exceptional position of PEG - PDADMAC / E30 among the PCC in Table 4 is confirmed by the results of SAX measurements represented in Figure 17. SAX measurements were carried out with the aqueous dispersion of the PCC, the solid after freeze-drying, and a film cast from a dimethyl acetamide solution at room temperature. The scattering pattern between the solid powder and the film are identical whereas that of the PCC dispersion shows, besides the much lower intensity, another distinct difference. The s^{-1} – values at positions a, c, d, h correspond to a sequence of $1 : \sqrt{3} : 2\sqrt{7}$ thus indicating a clear hexagonal ordering. Note, the

peak at position h appears only in the X-ray diagram of the aqueous dispersion. However, in the diagram of the solids the peaks b and e indicate an additional lamellar ordering as the s^{-1} values obey the sequence 1:2. From the s^{-1} – values of peaks a and b characteristic dimension of the corresponding structures can be estimated and an idea can be developed how the corresponding structures may look like (cf. Figure 18). It is very reasonable that these complexes resemble on a molecular level a bottlebrush as it is sketched in Figure 18. The characteristic spacing of the lamellae in the solids is about 2.5 nm whereas that of the hexagonal pattern is about 3.1 nm and 3.6 nm for the solids and the PCC dispersion, respectively. Note, the latter values indicate a swelling of the structures in the dispersed state.

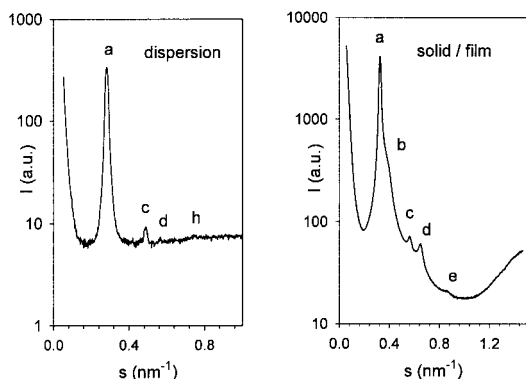


Figure 17: X-ray diagrams of the aqueous dispersion and solid / film of the PCC #3 in Table 4.

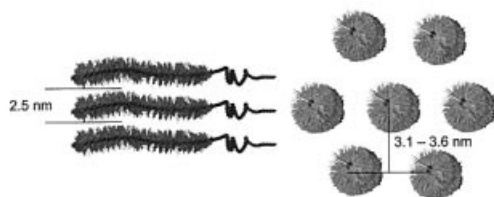


Figure 18: Sketch of the structural order for the PCC #3 estimated from SAX data; the backbone is the PEG-PDADMAC copolymer and the brushes are E30 (not to scale).

As already mentioned above, the PCC#2 that is made of PEG – PSS diblock copolymer and the cationic surfactant CTAB shows a different x-ray diffraction pattern. In this case the X-ray diagram of the solid shows only very weak indications of a lamellar structure with a characteristic length of about 3 nm. The reason for the disappearance of the hexagonal pattern is very likely the much higher molecular weight of the PSS block compared with the PDADMAC block. A GPC analysis of the complexes in dimethyl acetamide (with a PEG

calibration) revealed that the number average molecular weight of complex #2 and #3 is about $2.8 \cdot 10^7 \text{ g mol}^{-1}$ and $2.1 \cdot 10^5 \text{ g mol}^{-1}$, respectively. Of course, one has to be very careful with the absolute numbers but one can trust the tendency. Taking into account the molecular weight of the PEG block ($2 \cdot 10^3 \text{ g mol}^{-1}$) and the 1:1 complex formation these data indicate that also the molecular weight of both ionic blocks differs about a factor of 100. The longer the complex the higher is the probability of the appearance of disordered regions.

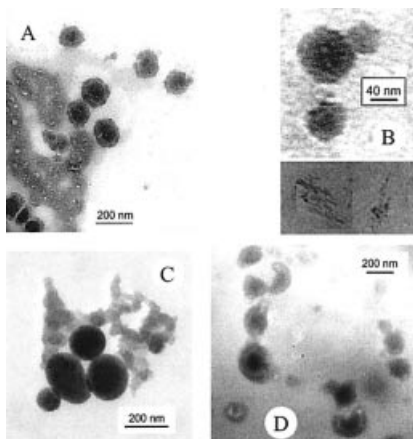


Figure 19: TEM pictures of PCC showing the various morphologies.

A, B – PEG - PDADMAC / E30 (#3)
C – PEG – PDADMAC / PEG – PSS (#5)
D – PEG – PDADMAC / PNIPAM – PAMPS

The PNIPAM – PAMPS is a statistical copolymer prepared by radical polymerization at 70°C with the following recipe: 100 g of water, 11 g of NIPAM, 4.5 g of AMPS, 0.3 g of VA086 as initiator.

Finally, the question arises concerning the look or the morphology of the individual particles of the PCC dispersions. The TEM pictures assembled in Figure 19 show a variety of morphologies and prove that there is obviously no necessity that these particles possess in any case a spherical shape.

A spherical shape and a smooth interface were always observed for PCC made of two block copolymers. An example is given in Figure 19 C for PEG – PDADMAC / PEG – PSS (PCC#5). But also for the PCC#1 and #4, which are supposed to be Janus – type, particles no special morphologies but only spherical particles are observed. It is absolutely logical that these PCC, due to the way they have been prepared, should have a hydrophilic shell consisting of two different hydrophilic polymers but obviously it is very hard or even impossible to prove this by TEM without special staining techniques. Contrary, if instead of the PSS – PNIPAM block copolymer a statistical copolymer PNIPAM – PAMPS is used as partner for PEG – PDADMAC the TEM pictures reveal a special morphology (cf. Figure

19 D). Only in this particular case half-moon like morphologies are observed that additionally possess a core shell structure. This seems to be reasonable because NIPAM units of the statistical copolymer should be more attached to the core and should not be able to phase separate, as it is possible for PNIPAM blocks.

The PCC#3 shows on the TEM pictures multiple morphology. Besides particles in the size range between less than 50 and 200 nm in diameter with a very broad size distribution (cf. Figure 19 A and upper part of B) also objects with a non-spherical morphologies appear (lower part of Figure 19 B). These non-spherical objects resemble somehow lamellar structures. The spherical particles show a core shell structure where the shell appears not smooth but exhibits a lot of indentations. Similar particles are also observed for the PCC#2. In conclusion, PCC are a new class of polymer dispersions that offers some interesting possibilities. For instance, the composition and the morphology of these particles can be altered almost at will. This seems to be very promising for future activities in several direction of research in the field of polymer colloid chemistry.

Acknowledgements

The authors acknowledge financial support from the Max Planck Society and are indebted to Mrs. B. Heilig, Mrs. S. Pirok, Mrs. R. Pitschke, Mrs. R. Rafler, Mrs. C. Remde, and Mrs. I. Zenke for analytical and preparative assistance. The interpretation of the X-ray data was mainly due to Dr. B. Smarsly whose help is gratefully acknowledged. For model calculations of density profiles and P-ratios the authors thank Dr. I. Müller.

References

1. A. S. Dunn, H. W. Melville *Nature* **169**, 699 (1952)
2. G. Mino, S. Kaizerman, E. Rasmussen *J. Amer. Chem. Soc.* **81**, 1494 (1959)
3. G. Odian "Principles of Polymerization", 3rd edition, Wiley, 1991, 220
4. G. Odian, J. H. T. Kho *J. Macromol. Sci. Chem.* **A-4**, 317 (1970)
5. K. Tauer *Polym. Adv. Technol.* **6**, 435 (1995)
6. L. Rosengarten, K. Tauer *Ber. Bunsenges. Phys. Chem.* **100**, 734 (1996)
7. K. Tauer, M. Antonietti, L. Rosengarten, H. Müller *Macromol. Chem. Phys.* **199**, 897 (1998)
8. The polymerizations have been carried out in water in a reaction calorimeter RM200 (ChemiSens AB, Lund, Sweden) as described in ⁹⁾ with the following recipes at 70 °C. A: 0.56 M N-isopropyl acryl amide, 0.096 M (monomer units) poly(styrene sulfonate) with terminal methylol groups and an mass average molecular weight of $4 \cdot 10^5$ g mol⁻¹

- that was prepared by radical polymerization of styrene sulfonate initiated with 2,2'-azobis[2-methyl-N-(2-hydroxyethyl)-propionamide] (VA-086 from Wako) in water at 70 °C, 0.002 M Ce^{4+} , and 0.1 M H^+ as nitric acid; B: 0.5 M N-isopropyl acryl amide, 0.01M poly(ethylene glycol) monomethylether with a molecular weight of 5000 g mol⁻¹, 0.01 M Ce^{4+} , and 0.1 M H^+ as nitric acid; C: same as B but without poly(ethylene glycol) monomethylether.
9. K. Tauer, H. Müller, C. Schellenberg, L. Rosengarten *Colloids Surfaces A: Physico-chem. Eng. Asp.* **153**, 143 (1999)
 10. M. D. C. Topp, PhD Thesis, University Twente, The Netherlands, 2000
 11. M. D. C. Topp, I. H. Leunen, P. J. Dijkstra, K. Tauer, C. Schellenberg, J. Feijen *Macromolecules* **33**, 4986 (2000)
 12. Polymerization recipe: PEG-monomethylether (molecular weight of 5000 g/mol) 5 g; 100 ml water, NIPAAM 35mmol; initiation by addition of 0,73 mmol ceric ammonium nitrate dissolved in 4 ml 1M nitric acid; T: 60°C.
 13. L. Rosengarten PhD thesis, MPI Colloids and Interfaces and University Potsdam, Germany, 1996
 14. The *terminus technicus* "micelle" is in the case of the PEG-PNIPAM block copolymers preferred in relation to "particles" because the PEG-PNIPAM micelles dissolve again at temperatures below the LCST thus illustrating an equilibrium situation, as it is known from classical micelle formation of surfactants.
 15. The polymerization recipe: 4 g of PSS (0.1 M with respect to the styrene sulfonates monomer), 0.22 g (0.002 M) of cerium ammonium nitrate, 1.26 – 0.32 g (0.055 – 0.014 M) of NIPAM, 200 g of water, 50 °C, 5.8 g (0.28 M) of styrene added 40 minutes after start of NIPAM polymerization with except run D where the styrene was added after 90 minutes. The styrene conversion was determined gravimetrically.
 16. $D_{1,0}$, $D_{1,3}$, $D_{3,3}$ are average diameters obtained from enumerating TEM pictures according to $D_{k,r} = \left[\frac{\sum_i n_i D_i^{k+r}}{\sum_i n_i D_i^r} \right]^{1/k}$ where $D_{1,0}$, $D_{1,3}$ and $D_{3,3}$ are the number average diameter, the weight average diameter, and an average diameter corresponding to light scattering, respectively; D_i – intensity weighted average particle size from dynamic light scattering; $\Delta R = 0.5(D_{1,3} - D_{3,3})$ – corona thickness.
 17. P. Pincus *Macromolecules* **24**, 2912 (1991)
 18. K. Tauer, H. Müller, L. Rosengarten, K. Riedelsberger *Colloids Surfaces A: Physicochem. Eng. Asp.* **153**, 75 (1999)
 19. The polymerization recipe was as follows: $4 \cdot 10^{-3}$ M of PEG-monomethylether with a molecular weight of $5 \cdot 10^3$ g mol⁻¹, 0.3 M of NIPAM, 0.3 M of MMA, $7 \cdot 10^{-3}$ cerium ammonium nitrate, 60 °C.
 20. J. Roovers "Dilute solution properties of regular star polymers" in "Star and hyper-branched polymers", M. K. Mishra; S. Kobayashi (eds), Marcel Dekker, New York, 1999
 21. M. Schmidt, D. Nерger, W. Burchhard *Polymer* **20**, 582 (1979)
 22. M. Antonietti, W. Bremser, M. Schmidt *Macromolecules* **23**, 3796 (1990)
 23. W. Burchard, M. Schmidt, W. H. Stockmayer *Macromolecules* **13**, 1265 (1980)
 24. C. Casagrande, P. Fabre, E. Raphaël, M. Veyssié *Europhys. Lett.* **9**, 251 (1989)
 25. P. G. de Gennes *Rev. Modern Phys.* **64**, 645 (1992)

26. K. Fujimoto, K. Nakahama, M. Shidara, H. Kawaguchi *Langmuir* **15**, 4630 (1999)
27. H. Ni, G. Ma, M. Nagai, S. Omi *J. Appl. Polym. Sci.* **76**, 1731 (2000)
28. The PEG - PDADMAC and the PEG – PSS diblock copolymers were prepared by radical polymerization of diallyl dimethyl ammonium chloride (180 g) and styrene sulfonate (170 g), respectively, in water (2000 g) with PEG-azo-initiators ⁷⁾ (30 g) with a molecular weight of the PEG of $2 \cdot 10^3 \text{ g mol}^{-1}$ at 70 °C.
29. B. Schwarz, G. Mönch, G. Ilgenfritz, R. Strey *Langmuir* **16**, 8643 (2000)